Pathologies in Lovelock AdS black branes and AdS/CFT

AUTHOR(S):

Takahashi, Tomohiro; Soda, Jiro

CITATION:

Takahashi, Tomohiro ...[et al]. Pathologies in Lovelock AdS black branes and AdS/CFT. Classical and Quantum Gravity 2012, 29(3): 35008.

ISSUE DATE:

2012-02-07

URL:

http://hdl.handle.net/2433/153406

Pathologies in Lovelock AdS Black Branes and AdS/CFT

Tomohiro Takahashi and Jiro Soda

Department of Physics, Kyoto University, Kyoto, 606-8502, Japan

(Dated: March 7, 2012)

Abstract

We study pathologies in AdS black branes in Lovelock theory. More precisely, we examine the conditions that AdS black branes have a naked singularity, ghost instability and dynamical instability. From the point of view of the AdS/CFT correspondence, pathologies in AdS black branes indicate pathologies in the corresponding CFT. Hence, in Lovelock theory, we need to be careful when we apply AdS/CFT to various phenomena such as the shear viscosity to entropy ratio in strongly coupled quantum field theory.

PACS numbers: 04.50.-h

I. INTRODUCTION

It is well known that AdS black branes play a central role in the application of the AdS/CFT correspondence to various phenomena such as condensed matter physics and fluid dynamics [1–3]. Remarkably, the AdS/CFT correspondence holds in any dimensions. In higher dimensions, however, a natural theory of gravity is not general relativity but Lovelock theory [4, 5]. Thus, it is natural to consider the AdS/CFT correspondence in the context of Lovelock theory.

The AdS/CFT correspondence in Lovelock theory has been already discussed in the context of the shear viscosity to entropy ratio. It is conjectured that the shear viscosity to entropy ratio η/s is larger than $1/4\pi$, which is called the KSS bound [6]. Recently, in the case that the dual gravitational theory is Lovelock theory, this ratio has been calculated as $\eta/s = (1-2\alpha_2)/4\pi$, where α_2 is an appropriately normalized second order Lovelock coefficient [7]. It seems that the KSS bound is violated for a positive α_2. However, when we take into account pathologies in AdS black branes, α_2 must be somewhat restricted. Indeed, there are several works on the causality violation of AdS black branes in conjunction with the KSS bound [8–10]. Clearly, it is important to clarify pathologies in AdS black branes.

In this paper, we consider pathologies in AdS black brane solutions in Lovelock theory. First, we explain our method using analytically tractable cases in 5-dimensions and 6-dimensions. In other dimensions, we have to resort to numerical analysis. As typical examples, we numerically study pathologies in AdS black branes in 10-dimensions and 11-dimensions. In recent work, this issue has been investigated in [11] based on the master equations derived by us [12]. They used near horizon analysis in the most part of their work and alluded to the importance of the bulk geometry based on numerical results. However, they have never given general conditions for the occurrence of pathologies. In this paper, we explicitly present the conditions for the occurrence of pathologies. Using the conditions, we will give detailed analysis of pathologies in Lovelock AdS black branes and discuss its implications in AdS/CFT.

The organization of this paper is as follows. In section II, we review Lovelock theory and explain a graphical method for constructing black brane solutions. In section III, we clarify the conditions for avoiding a naked singularity, ghost instability and dynamical instability. In section IV, we analytically study pathologies in AdS black branes in 5-dimensions and

6-dimensions. In section V, we numerically examine pathologies in AdS black branes in 10-dimensions and 11-dimensions. In section VI, based on the analytical and numerical results, we discuss implications of our findings in the AdS/CFT correspondence. The final section VII is devoted to conclusion.

II. LOVELOCK ADS BLACK BRANES

In this section, we review Lovelock theory and introduce a graphical method for constructing AdS black brane solutions.

The most general divergence free symmetric tensor constructed out of a metric and its first and second derivatives was obtained by Lovelock [4]. The corresponding Lagrangian can be constructed from m-th order Lovelock terms

$$\mathcal{L}_m = \frac{1}{2^m}\delta^{\lambda_1\sigma_1\cdots\lambda_m\sigma_m}_{\rho_1\kappa_1\cdots\rho_m\kappa_m} R_{\lambda_1\sigma_1}{}^{\rho_1\kappa_1}\cdots R_{\lambda_m\sigma_m}{}^{\rho_m\kappa_m} \ , \tag{1}$$

where $R_{\lambda\sigma}{}^{\rho\kappa}$ is the Riemann tensor in D-dimensions and $\delta^{\lambda_1\sigma_1\cdots\lambda_m\sigma_m}_{\rho_1\kappa_1\cdots\rho_m\kappa_m}$ is the generalized totally antisymmetric Kronecker delta defined by

$$\delta^{\mu_1\mu_2\cdots\mu_p}_{\nu_1\nu_2\cdots\nu_p} = \det\begin{pmatrix} \delta^{\mu_1}_{\nu_1} & \delta^{\mu_1}_{\nu_2} & \cdots & \delta^{\mu_1}_{\nu_p} \\ \delta^{\mu_2}_{\nu_1} & \delta^{\mu_2}_{\nu_2} & \cdots & \delta^{\mu_2}_{\nu_p} \\ \vdots & \vdots & \ddots & \vdots \\ \delta^{\mu_p}_{\nu_1} & \delta^{\mu_p}_{\nu_2} & \cdots & \delta^{\mu_p}_{\nu_p} \end{pmatrix} .$$

By construction, the Lovelock terms vanish for $2m > D$. It is also known that the Lovelock term with $2m = D$ is a topological term. Thus, Lovelock Lagrangian in D-dimensions is defined by

$$\mathcal{L} = \sum_{m=0}^{k} c_m \mathcal{L}_m \ , \tag{2}$$

where we defined the maximum order $k \equiv [(D-1)/2]$ and c_m are arbitrary constants. Here, $[z]$ represents a maximum integer satisfying $[z] \leq z$. Taking variation of the Lagrangian with respect to the metric, we can derive Lovelock equations

$$0 = \sum_{m=0}^{k} c_m \delta^{\nu\lambda_1\sigma_1\cdots\lambda_m\sigma_m}_{\mu\rho_1\kappa_1\cdots\rho_m\kappa_m} R_{\lambda_1\sigma_1}{}^{\rho_1\kappa_1}\cdots R_{\lambda_m\sigma_m}{}^{\rho_m\kappa_m} \ . \tag{3}$$

Hereafter, we set $c_0 = (D-1)(D-2)\lambda$ $(\lambda > 0)$, $c_1 = 1$ and $c_m = \alpha_m / \left\{ m\lambda^{m-1} \prod_{p=1}^{2m-2}(D-2-p) \right\}$ $(m \geq 2)$ for convenience. Note that the coefficients α_m are dimensionless.

It is well known that there exist static exact solutions of the Lovelock equations (3) [13–15]. Let us consider the following metric

$$ds^2 = r^2\psi(r)dt^2 + \frac{dr^2}{-r^2\psi(r)} + r^2\delta_{ij}dx^i dx^j \ . \tag{4}$$

We assume that $\psi(r)$ is negative outside of the horizon. Substituting this metric ansatz into Eq.(3), we can obtain an algebraic equation for $\psi(r)$:

$$W[\psi] \equiv \sum_{m=2}^{k} \left(\frac{\alpha_m}{m} \psi^m \right) + \psi + 1 = \frac{\mu}{r^{D-1}} \ , \tag{5}$$

where μ is a constant of integration which is related to the ADM mass and we assume it is positive. Note that we fixed the scale by setting $\lambda = 1$ in Eq.(5).

Now, we explain how to construct solutions using a graphical method [16, 17]. Apparently, W must be positive. In general, there are many branches. In Fig.1, we depicted $y = W[\psi]$ and $y = \mu/r^{D-1}$ with r fixed in $\psi - y$ plane. The intersection of the curve and the line determines ψ once r is given. By varying r, we obtain the solution of Eq.(5). Taking a look at the metric (4), we see that the horizon corresponds to $\psi = 0$. Hence, a black brane corresponds to the branch containing $\psi = 0$. Next, consider the asymptotic infinity $r \to \infty$ or $y = \mu/r^{D-1} \to 0$, the function $\psi(r)$ in Fig.1 approaches ψ_a which is the largest negative root of $W[\psi] = 0$. Thus, the curve between $\psi = \psi_a$ and $\psi = 0$ defines a black brane solution.

III. PATHOLOGIES

In this section, we list up pathologies in Lovelock AdS black branes. In particular, we reveal the conditions for the occurrence of pathologies.

A. Naked Singularity

In the graphical method, it is easy to find singularities. Let us recall the Kretschmann invariant which is calculated as

$$R_{\mu\nu\rho\lambda}R^{\mu\nu\rho\lambda} = (\partial_r^2(r^2\psi))^2 + 2(D-2)\frac{(\partial_r(r^2\psi))^2}{r^2} + 2(D-2)(D-3)\psi^2 \ . \tag{6}$$

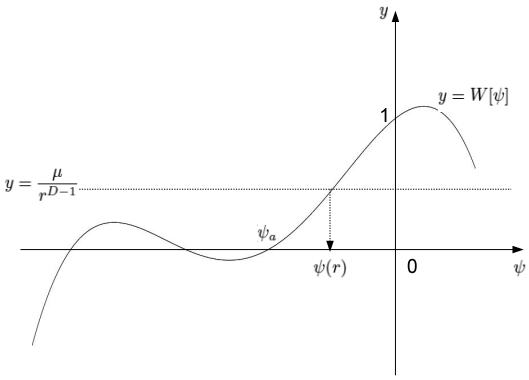

FIG. 1: A curve $y = W[\psi]$ and a line $y = \mu/r^{D-1}$ are depicted in $\psi - y$ plane. Note that r should be regarded as a constant when we draw this figure. The intersection of the curve and the line determines a solution of Eq.(5). Here, ψ_a is defined as the largest negative root of $W[\psi] = 0$.

If this invariant diverges, there exist singularities. This occurs at $r = 0$ and the point where $\partial_r\psi$ diverges. In fact, $\partial_r\psi$ diverges when $W[\psi]$ becomes extremal value because of a relation $\partial_r\psi = -(D-1)W[\psi]/(r\partial_\psi W)$ obtained from (5). Since $\partial_\psi W|_{\psi=0} = 1 > 0$, if $W[\psi]$ is a monotonically increasing function in the region $[\psi_a,\ 0]$, there is no naked singularity. Fig.2-(a) corresponds to this case. However, like in Fig.2-(b), if $W[\psi]$ has an extremal point between ψ_a and 0, there exists a naked singularity. Note that the shape of $W[\psi]$ depends only on Lovelock coefficients α_m, so whether a branch has a naked singularity or not is determined by these constants. Since we want to avoid the naked singularity, we have to exclude the solutions which have extrema between $\psi = \psi_a$ and $\psi = 0$. Note that there maybe exotic cases for which ψ_a does not exist. These solutions should be excluded because they necessarily have the naked singularity.

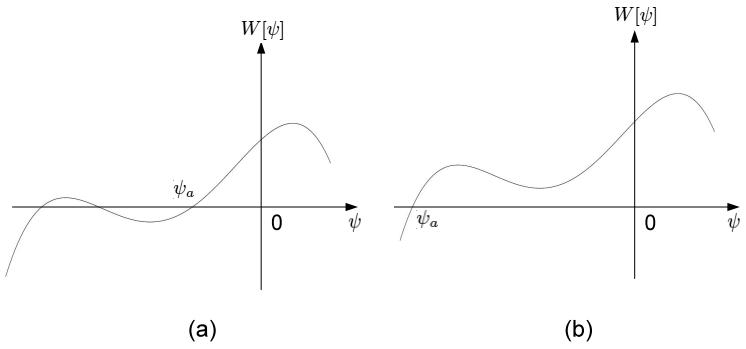

FIG. 2: (a) Apparently, $W[\psi]$ has no extremal point in the region $[\psi_a,\ 0]$. Hence, there is no naked singularity in this case. (b) There is an extremal point. Thus, there exists a naked singularity.

B. Ghost Instability

In Lovelock theory, the sign in front of the kinetic term in the action could be negative, namely the ghost instability could occur. In the previous paper [12], we have shown that there exists the ghost instability when

$$K[\psi] \equiv (D-3)(\partial_\psi W)^2 - (D-1)W\partial_\psi^2 W \tag{7}$$

becomes negative. Hence, we need to check the sign of $K[\psi]$ to check if a black brane has the ghost instability or not.

C. Dynamical Instability

As we have shown in [12], the function $W(\psi)$ determines if the dynamical instability of Lovelock black branes occurs. Using the symmetry of the planar part of the metric, we can classify metric perturbations into the scalar, vector, tensor sectors. In the absence of the ghost instability, we can prove that there is no dynamical instability in the vector sector [12].

There exist the dynamical instability for tensor sector when

$$\begin{aligned} L[\psi] \equiv\ & (D-3)(D-4)\left(\partial_\psi W\right)^4 - (D-1)(D-6)W\left(\partial_\psi W\right)^2\partial_\psi^2 W \\ & +(D-1)^2W^2\left\{\partial_\psi W\partial_\psi^3 W - (\partial_\psi^2 W)^2\right\}\ , \end{aligned} \tag{8}$$

is negative [12, 16]. Similarly, there exist the dynamical instability for scalar sector, when

$$\begin{aligned} M[\psi] \equiv\ & (D-2)(D-3)(\partial_\psi W)^4 - 3(D-2)(D-1)W\partial_\psi^2 W(\partial_\psi W)^2 \\ & +(D-1)^2W^2\left\{3(\partial_\psi^2 W)^2 - \partial_\psi W\partial_\psi^3 W\right\}. \end{aligned} \tag{9}$$

is negative [12]. In both cases, the square of the effective speed of sound becomes negative. This kind of instability is found in the cosmological context for the first time [18].

In order to find the dynamical instability, what we have to check is the sign of $L[\psi]$ and $M[\psi]$ in the region $\psi_a < \psi < 0$. Note that these functions and ψ_a is independent of μ, hence whether the dynamical instability exist or not depends only on Lovelock coefficients α_m.

IV. PATHOLOGY INSPECTION: ANALYTIC RESULTS

In this section, we analytically investigate pathologies in 5-dimensions and 6-dimensions for which we have $k = 2$. In these cases, W is given by

$$W[\psi] = \frac{\alpha_2}{2}\psi^2 + \psi + 1 \ , \qquad \alpha_2 \neq 0 \ . \tag{10}$$

This can be written as

$$W = \frac{\alpha_2}{2}\left(\psi + \frac{1}{\alpha_2}\right)^2 + 1 - \frac{1}{2\alpha_2} \tag{11}$$

from which we see that there is no solution for $W = 0$ if $\alpha_2 > 1/2$. Since there is an extremum in the region $\psi < 0$, we have a naked singularity in these cases. Thus, only the range $\alpha_2 \leq 1/2$ is allowed.

For $\alpha_2 \leq 1/2$, there are solutions for $W = 0$

$$\psi_W = \frac{-1 \pm \sqrt{1 - 2\alpha_2}}{\alpha_2} \ . \tag{12}$$

We have defined ψ_a as the largest negative root. In the cases $0 < \alpha_2 \leq 1/2$, the largest negative root should be

$$\psi_a = \frac{-1 + \sqrt{1 - 2\alpha_2}}{\alpha_2} \ . \tag{13}$$

In the cases $\alpha_2 < 0$, that becomes

$$\psi_a = \frac{-1 + \sqrt{1 - 2\alpha_2}}{\alpha_2} = \frac{1 - \sqrt{1 + 2|\alpha_2|}}{|\alpha_2|} \ . \tag{14}$$

In any case, the plus sign in (12) corresponds to ψ_a. Thus, we do not have any naked singularity as long as $\alpha_2 \leq 1/2$.

Next, let us see if we have ghosts. To this aim, we need to look at the sign of $K[\psi]$. In 5-dimensions or 6-dimensions, we obtain

$$K = \begin{cases} 2(1 - 2\alpha_2) & (\text{for } D = 5) \\ (\alpha_2\psi + 1)^2/2 + 5(1 - 2\alpha_2)/2 & (\text{for } D = 6) \end{cases} \tag{15}$$

Apparently, the condition for no naked singularity $\alpha_2 \leq 1/2$ guarantees $K \geq 0$. Hence, we do not have ghosts as long as we do not have naked singularities in 6-dimensions. In 5-dimensions, for $\alpha_2 = 1/2$, K vanishes, which is singular. Hence, we have the condition $\alpha_2 < 1/2$ in 5-dimensions.

From now on, we check the stability of black branes in tensor and scalar sectors. The analysis depends on the dimensions. Hence, we discuss the stability in 5 and 6 dimensions, separately.

A. 5-dimensions

First, we discuss the stability in the tensor sector by looking at the sign of L. From the definition (8), L can be calculated as

$$L = 2(1-2\alpha_2)\left\{3\alpha_2^2\psi^2 + 6\alpha_2\psi + (1+4\alpha_2)\right\} \ . \tag{16}$$

We see that there exist instability for $\alpha_2 < -1/4$ because $L[0] < 0$ in this range. Then, we consider the remaining range $-1/4 \leq \alpha_2 < 1/2$. In this case, $L = 0$ has solutions

$$\psi_{L\pm} = \frac{-1 \pm \sqrt{2/3}\sqrt{1-2\alpha_2}}{\alpha_2} \ . \tag{17}$$

Comparing these solutions with ψ_a, we see $\psi_a > \psi_{L\pm}$ in the range $0 < \alpha_2 < 1/2$ and $\psi_a < 0 < \psi_{L\pm}$ in the range $-1/4 \leq \alpha_2 < 0$. Thus, in the range $[\psi_0, 0]$, we always have $L > 0$ for $0 < \alpha_2 < 1/2$ and $-1/4 \leq \alpha_2 < 0$.

Next, we study the stability in the scalar sector. From the definition (9), $M[\psi]$ is given by

$$M[\psi] = 6(1-2\alpha_2)\left(-\alpha_2^2\psi^2 - 2\alpha_2\psi + (1-4\alpha_2)\right) \ . \tag{18}$$

For $1/4 < \alpha_2 < 1/2$, we have $M[0] < 0$ and then there is the instability. Thus, we need to check the range $\alpha_2 \leq 1/4$ in the following. It is easy to see that $M = 0$ have solutions

$$\psi_{M\pm} = \frac{-1 \pm \sqrt{2}\sqrt{1-2\alpha_2}}{\alpha_2} \ . \tag{19}$$

Comparing these solutions with ψ_a, we find $\psi_- < \psi_a < 0 < \psi_+$ for $0 < \alpha_2 \leq 1/4$, and $\psi_+ < \psi_a < 0 < \psi_-$ for $\alpha_2 < 0$. Therefore, in the range $[\psi_a, 0]$, we conclude $M \geq 0$ for $0 < \alpha_2 \leq 1/4$ and $\alpha_2 < 0$.

Combining the above results, we found that black branes in 5-dimensions have no pathology for the range $-1/4 \leq \alpha_2 \leq 1/4$, where the trivial case $\alpha_2 = 0$ is included.

B. 6-dimensions

Now, we investigate pathologies in AdS black branes in 6-dimensions. First, we check the stability in the tensor sector. In 6-dimensions, $L[\psi]$ becomes

$$L[\psi] = -\frac{\alpha_2^4}{4}\psi^4 - \alpha_2^3\psi^3 + (11 - 25\alpha_2)\alpha_2^2\psi^2 + 24\alpha_2\psi - 50\alpha_2^2\psi + (6 - 25\alpha_2^2) \tag{20}$$

From this expression, we can conclude $L[0] < 0$ for $\alpha_2 < -\frac{\sqrt{6}}{5}$, $\frac{\sqrt{6}}{5} < \alpha_2 \leq \frac{1}{2}$. Hence, in order not to have the instability in the tensor sector, we have to choose a parameter in the range $-\sqrt{6}/5 \leq \alpha_2 \leq \sqrt{6}/5$, where $\alpha_2 = 0$ is a trivial case. Notice that the equation $L = 0$ have four solutions

$$\psi_{L\pm\pm} = -\frac{1}{\alpha_2} \pm \frac{\sqrt{1 - 2\alpha_2}}{\alpha_2}\left(\sqrt{15} \pm \sqrt{10}\right) \ . \tag{21}$$

Here, $\psi_{L\pm\pm}$ distinguish four possible solutions. Comparing these solutions with ψ_a, we find that

$$\psi_{L-+} < \psi_{L--} < \psi_{L+-} < \psi_a < 0 < \psi_{L++} \tag{22}$$

for $0 < \alpha_2 < \sqrt{6}/5$, and we have

$$\psi_{L++} < \psi_a < 0 < \psi_{L+-} < \psi_{L--} < \psi_{L-+} \tag{23}$$

for $-\sqrt{6}/5 < \alpha_2 < 0$. Thus, we see $L > 0$ in the range $[\psi_a, 0]$.

Remarkably, $M[\psi]$ can be written as

$$M[\psi] = \frac{3}{4}\left(-4 + 10\alpha_2 + 2\alpha_2\psi + \alpha_2^2\psi^2\right)^2 \tag{24}$$

Hence, there exists no instability in the scalar sector.

To conclude, there exists no pathology in AdS black branes in 6-dimensions as long as we take a parameter in the range $-\sqrt{6}/5 \leq \alpha_2 \leq \sqrt{6}/5$.

V. PATHOLOGY INSPECTION: NUMERICAL APPROACH

Now, we are in a position to examine the pathologies in AdS black branes numerically. In this paper, we consider 10-dimensions and 11-dimensions because the analysis and the results in other dimensions are similar. Our strategy is very simple. For each coefficients α_m, we search for ψ_a and check the sign of $\partial_\psi W$, $K[\psi]$, $L[\psi]$ and $M[\psi]$ in the region $\psi_a < \psi < 0$. The mesh size of this calculation is $\Delta\alpha_m = 0.05$. We have checked our numerical method can reproduce the analytical results in 5-dimensions and 6-dimensions.

A. 10-dimensions

In 10-dimensions, the Lovelock black holes can be characterized by the functional

$$W[\psi] = \frac{\alpha_4}{4}\psi^4 + \frac{\alpha_3}{3}\psi^3 + \frac{\alpha_2}{2}\psi^2 + \psi + 1 \ . \tag{25}$$

Substituting this expression into $\partial_\psi W[\psi]$, (7), (8), and (9), we can find forbidden region in 3-dimensional parameter space $\{\alpha_2, \alpha_3, \alpha_4\}$. In Fig.3, we plot forbidden regions due to various reasons in $\alpha_2 - \alpha_3$ plane with $\alpha_4 = -1.5,\ 0,\ 0.5$, respectively. Interestingly, there is a region where both scalar and tensor sector instability exist. The shaded region represents an allowed region.

In Fig.3, when $\alpha_4 = 0$, the border between the allowed region and the unstable region due to the scalar sector instability can be obtained from the condition $M[0] = 0$ as

$$\alpha_3 = \frac{3}{2}\alpha_2^2 - \frac{3(D-2)}{2(D-1)}\alpha_2 + \frac{(D-2)(D-3)}{2(D-1)^2} \tag{26}$$

Similarly, the border between the allowed region and the unstable region due to the tensor sector instability can be determined by the condition $L[0] = 0$ as

$$\alpha_3 = \frac{\alpha_2^2}{2} + \frac{D-6}{2(D-1)}\alpha_2 - \frac{(D-3)(D-4)}{2(D-1)^2} \ . \tag{27}$$

These analytical results are in good agreement with our numerical results. Thus, we see that these dynamical instabilities occur near the horizon because $\psi = 0$ corresponds to the horizon. These results are consistent with those obtained in [11]. Note that $M[0]$ and $L[0]$ are determined by α_2 and α_3 and so these borders are independent of α_4 if instabilities occur near the horizon. However, comparing three figures in Fig.3, the region where black holes are unstable under scalar perturbations for $\alpha_4 = -1.5$ is very different from that for $\alpha_4 = 0,\ 0.5$. This suggests that these instabilities occur away from the horizon. Therefore, α_4 affects the behavior of $M[\psi]$ and change the allowed region in $\alpha_2 - \alpha_3$ plane. Indeed, this fact can be understood more easily from Fig.4. In Fig.4, we plot forbidden regions in $\alpha_2 - \alpha_4$ plane with $\alpha_3 = -0.2,\ 0,\ 0.5$, respectively. In these figures, we see vertical stripes for negative α_4. For example, in Fig.4 with $\alpha_3 = 0$, there are three vertical lines: $\alpha_2 \simeq -1,\ \alpha_2 \simeq 0.5,\ \alpha_2 \simeq 0.75$. These lines can be obtained from $L[0] = 0$ as

$$\alpha_2 = -\frac{D-6}{2(D-1)} \pm \sqrt{2\alpha_3 + \frac{5D^2 - 40D + 84}{4(D-1)^2}} \tag{28}$$

and from $K[0] = 0$ as

$$\alpha_2 = \frac{D-3}{D-1} \ . \tag{29}$$

This agreement between the analytical and numerical results is remarkable. However, when α_4 becomes large, the stripe structure collapses. This suggests instabilities are not originated from the near horizon geometry. It turned out that α_4 is a relevant parameter for AdS black branes.

B. 11-dimensions

In 11-dimensions, the key functional is given by

$$W[\psi] = \frac{\alpha_5}{5}\psi^5 + \frac{\alpha_4}{4}\psi^4 + \frac{\alpha_3}{3}\psi^3 + \frac{\alpha_2}{2}\psi^2 + \psi + 1 \ . \tag{30}$$

Again, substituting this expression into $\partial_\psi W[\psi]$, (7), (8), and (9), we can find forbidden region in 4-dimensional parameter space $\{\alpha_2, \alpha_3, \alpha_4, \alpha_5\}$. Of course, it is a formidable task to visualize such a higher dimensional space. Hence, we look at several sections in the parameter space. In Fig. 5, we plot forbidden regions in $\alpha_2 - \alpha_5$ plane with $(\alpha_3,\ \alpha_4) = (0,\ 0)$, $\alpha_3 - \alpha_5$ plane with $(\alpha_2,\ \alpha_4) = (0,\ 0)$ and $\alpha_4 - \alpha_5$ plane with $(\alpha_2,\ \alpha_3) = (0,\ 0)$, respectively.

From these figures, we see that α_5 affects the allowed ranges of α_2, α_3 and α_4. In particular, in the case of $\alpha_3 - \alpha_5$ and $\alpha_4 - \alpha_5$ planes, the allowed region is finite. It indicates that AdS black branes in Lovelock theory are pathological in most cases.

VI. IMPLICATIONS IN ADS/CFT

Let us discuss implications of our results in the AdS/CFT correspondence.

With the master equation in [16], the shear viscosity to entropy ratio η/s has been calculated as

$$\frac{\eta}{s} = \frac{1}{4\pi}\left(1 - \frac{D-1}{D-3}\alpha_2\right)$$

through AdS/CFT correspondence [7]. Note that this depends only on α_2. Hence, it seems that α_3, α_4 and α_5 do not affect this value. However, as our numerical calculations have

shown, α_3, α_4 and α_5 affect the allowed region of α_2. This fact was also noticed in [11]. In 5-dimensions and 6-dimensions, the KSS bounds are lowered to $\eta/s = 1/8\pi$ and $\eta/s \simeq 0.59/4\pi$, respectively. Interestingly, in 10-dimensions , we see from Fig.3 that a positive α_2 is not allowed for any α_3 if $\alpha_4 = -1.5$. This means that the bound of η/s must be larger than $1/4\pi$ if $\alpha_4 = -1.5$. As another example, we can take $\alpha_4 = 0$ and $\alpha_3 = 0.5$, then the maximal value of α_2 is about -0.1. While if we take $\alpha_4 = 0.5$, the maximal α_2 becomes 0.15 at which $\alpha_3 = 0.2$. Thus, it turned out that the KSS like bound is sensitive to Lovelock coefficients.

It is also possible to apply our results to holographic superconductors [19]. There, the universality for the ratio between the frequency dependent conductivity and the critical temperature is found [20]. In Gauss-Bonnet theory, it is pointed out that this universality in holographic superconductors is violated for a large α_2 [21]. However, it is probable that this violation is due to the pathologies discussed in this paper. It would be interesting to extend holographic superconductors to Lovelock theory to clarify this point.

VII. CONCLUSION

We have discussed the pathologies in AdS black branes in Lovelock theory, analytically in 5-dimensions and 6-dimensions, and numerically in 10-dimensions and 11-dimensions. We obtained the general conditions for Lovelock coefficients α_m that these black branes have the naked singularity, the ghost instability, and the dynamical instability. It turned out that the dynamical instability could occur away from the horizon in contrast to a naive expectation. Thus, α_4 and α_5 also control the allowed region of α_2, and consequently changes the lower limit of η/s. We have also pointed out that the pathologies we have found could affect the interpretation of higher dimensional holographic superconductors.

In this paper, we did not consider the causality violation discussed in [8–11]. It is easy to take into account the causality violation based on the master equations [12]. Then, we could further restrict the allowed region for α_2. It is also straightforward to extend our analysis to other dimensions using the master equations [12].

Acknowledgments

We wish to thank Keiju Murata for fruitful discussions. This work was supported in part by the Grant-in-Aid for Scientific Research Fund of the Ministry of Education, Science and Culture of Japan No.22540274, the Grant-in-Aid for Scientific Research (A) (No.21244033, No.22244030), the Grant-in-Aid for Scientific Research on Innovative Area No.21111006, JSPS under the Japan-Russia Research Cooperative Program, the Grant-in-Aid for the Global COE Program "The Next Generation of Physics, Spun from Universality and Emergence".

---

[1] S. A. Hartnoll, arXiv:0903.3246 [hep-th].

[2] C. P. Herzog, arXiv:0904.1975 [hep-th].

[3] G. T. Horowitz, arXiv:1002.1722 [hep-th].

[4] D. Lovelock, J. Math. Phys. **12** (1971) 498.

[5] C. Charmousis, Lect. Notes Phys. **769**, 299 (2009) [arXiv:0805.0568 [gr-qc]].

[6] P. Kovtun, D. T. Son and A. O. Starinets, Phys. Rev. Lett. **94**, 111601 (2005) [arXiv:hep-th/0405231].

[7] X. H. Ge, S. J. Sin, S. F. Wu and G. H. Yang, Phys. Rev. D **80**, 104019 (2009) [arXiv:0905.2675 [hep-th]];
F. W. Shu, Phys. Lett. B **685**, 325 (2010) [arXiv:0910.0607 [hep-th]].

[8] M. Brigante, H. Liu, R. C. Myers, S. Shenker and S. Yaida, Phys. Rev. Lett. **100**, 191601 (2008) [arXiv:0802.3318 [hep-th]].

[9] J. de Boer, M. Kulaxizi and A. Parnachev, JHEP **1006**, 008 (2010) [arXiv:0912.1877 [hep-th]].

[10] X. O. Camanho and J. D. Edelstein, JHEP **1006**, 099 (2010) [arXiv:0912.1944 [hep-th]].

[11] X. O. Camanho, J. D. Edelstein and M. F. Paulos, JHEP **1105**, 127 (2011) [arXiv:1010.1682 [hep-th]].

[12] T. Takahashi and J. Soda, Prog. Theor. Phys. **124**, 711 (2010) [arXiv:1008.1618 [gr-qc]];
T. Takahashi and J. Soda, Prog. Theor. Phys. **124**, 911 (2010) [arXiv:1008.1385 [gr-qc]].

[13] J. T. Wheeler, Nucl. Phys. B **273**, 732 (1986).

[14] R. G. Cai, Phys. Rev. D **65**, 084014 (2002) [arXiv:hep-th/0109133].

[15] S. Nojiri and S. D. Odintsov, Phys. Lett. B **521**, 87 (2001) [Erratum-ibid. B **542**, 301 (2002)] [arXiv:hep-th/0109122].

[16] T. Takahashi and J. Soda, Phys. Rev. D **80**, 104021 (2009) [arXiv:0907.0556 [gr-qc]]; T. Takahashi and J. Soda, Phys. Rev. D **79**, 104025 (2009) [arXiv:0902.2921 [gr-qc]].

[17] X. O. Camanho and J. D. Edelstein, arXiv:1103.3669 [hep-th].

[18] S. Kawai, M. a. Sakagami and J. Soda, Phys. Lett. B **437**, 284 (1998) [arXiv:gr-qc/9802033]; S. Kawai and J. Soda, Phys. Lett. B **460**, 41 (1999) [arXiv:gr-qc/9903017].

[19] S. A. Hartnoll, C. P. Herzog and G. T. Horowitz, Phys. Rev. Lett. **101**, 031601 (2008) [arXiv:0803.3295 [hep-th]].

[20] G. T. Horowitz and M. M. Roberts, Phys. Rev. D **78**, 126008 (2008) [arXiv:0810.1077 [hep-th]].

[21] R. Gregory, S. Kanno and J. Soda, JHEP **0910**, 010 (2009) [arXiv:0907.3203 [hep-th]].

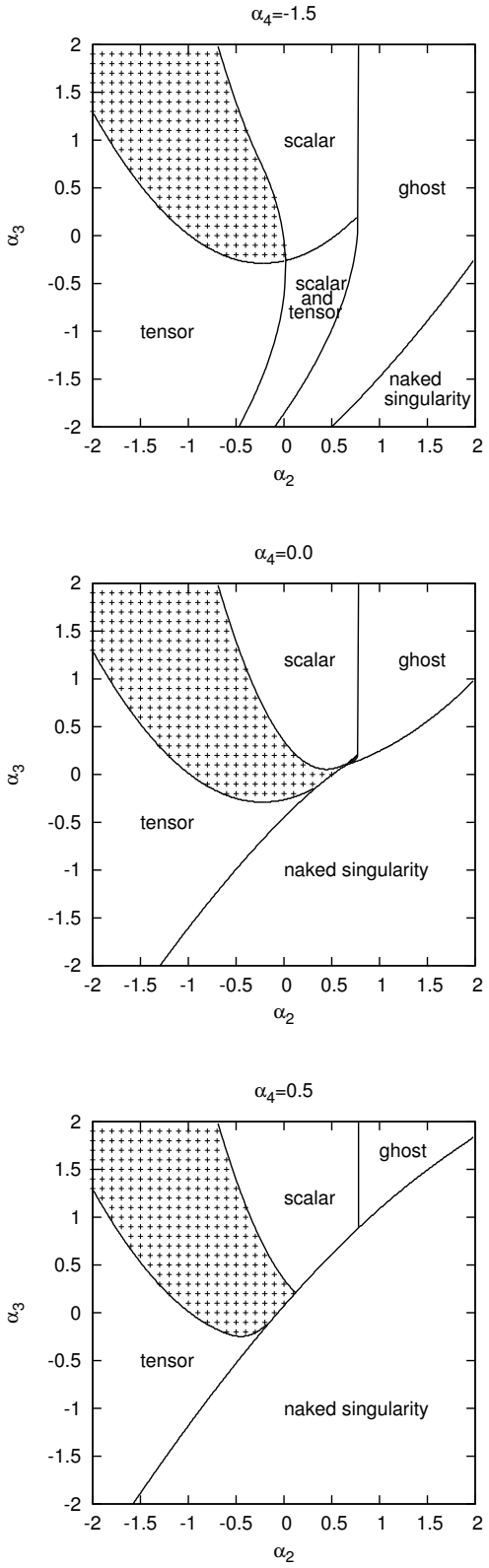

FIG. 3: We plot allowed and forbidden regions in $\alpha_2 - \alpha_3$ plane with $\alpha_4 = -1.5,\ 0,\ 0.5$ respectively. The shaded region represents an allowed region.

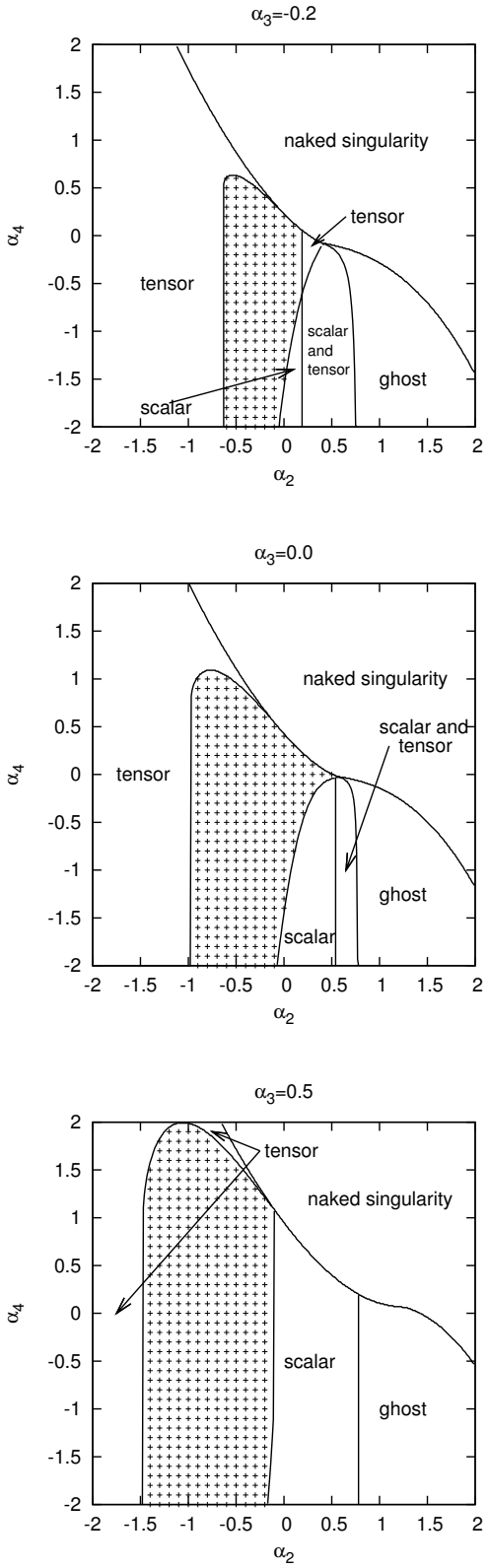

FIG. 4: We plot allowed and forbidden regions in $\alpha_2 - \alpha_4$ plane with $\alpha_3 = -0.2,\ 0,\ 0.5$ respectively. The shaded region represents an allowed region.

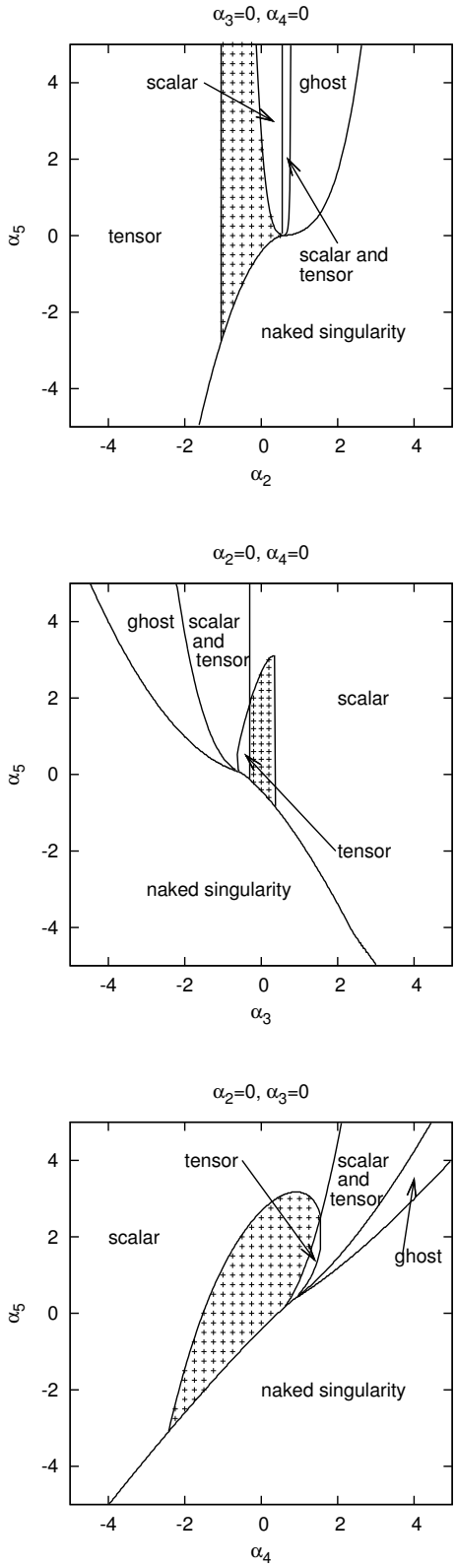

FIG. 5: We plot allowed and forbidden regions in $\alpha_2 - \alpha_5$, $\alpha_3 - \alpha_5$ and $\alpha_4 - \alpha_5$ planes, respectively. The shaded region represents an allowed region. In these figures, we set other Lovelock coefficients to be 0.